

Introduction

Assam-Arakan Basin comprises Cenozoic sedimentary successions, located in northeastern India is juxtaposed to both the Himalaya and Indo-Burman Ranges (IBR). The present day Brahmaputra river, flowing north and west of the Shillong Plateau is the only major drainage in the Assam Basin. The available studies explain its drainage course initially as paleo- Brahmaputra, flowing east of the Shillong Plateau, draining Assam Basin and reached to the Bengal Basin (Johnson and Alam 1991; Uddin and Lundberg 1999; Bracciali et al., 2015; Najman et al., 2008; 2016). It has been recommended that the modern drainage configuration of the Brahmaputra river occurred in response to Shillong Plateau uplift and Indo-Burman Ranges (IBR) westward propagation that caused the deflection of the paleo- Brahmaputra river course. However, unequivocal evidence of paleo- Brahmaputra remains enigmatic. Tipam sandstone and the overlying younger Dupi-Tila/Namsang/Dihing fluvial units of Assam-Arakan Basin are stratigraphically comparable to Subansiri and Kimin Formations of Siwalik foreland basin. Therefore, it raises a question on the river system that deposited these fluvial deposits in both the foreland basins.

The present study demonstrates the provenance for the fluvial sedimentary units of the Assam-Arakan Basin using petrography, heavy mineral distributions and detrital zircon U-Pb geochronology. X-ray Diffraction (XRD) and Electron Probe Micro Analyzer (EPMA) analyses were employed to correctly identify the heavy mineral species and support the semi-quantitative analysis of heavy minerals in the basin. The outcome of the study provides new insights towards the paleo- drainage evolution of the river course accountable for the fluvial sedimentation in the Assam-Arakan Basin.

Field Photographs

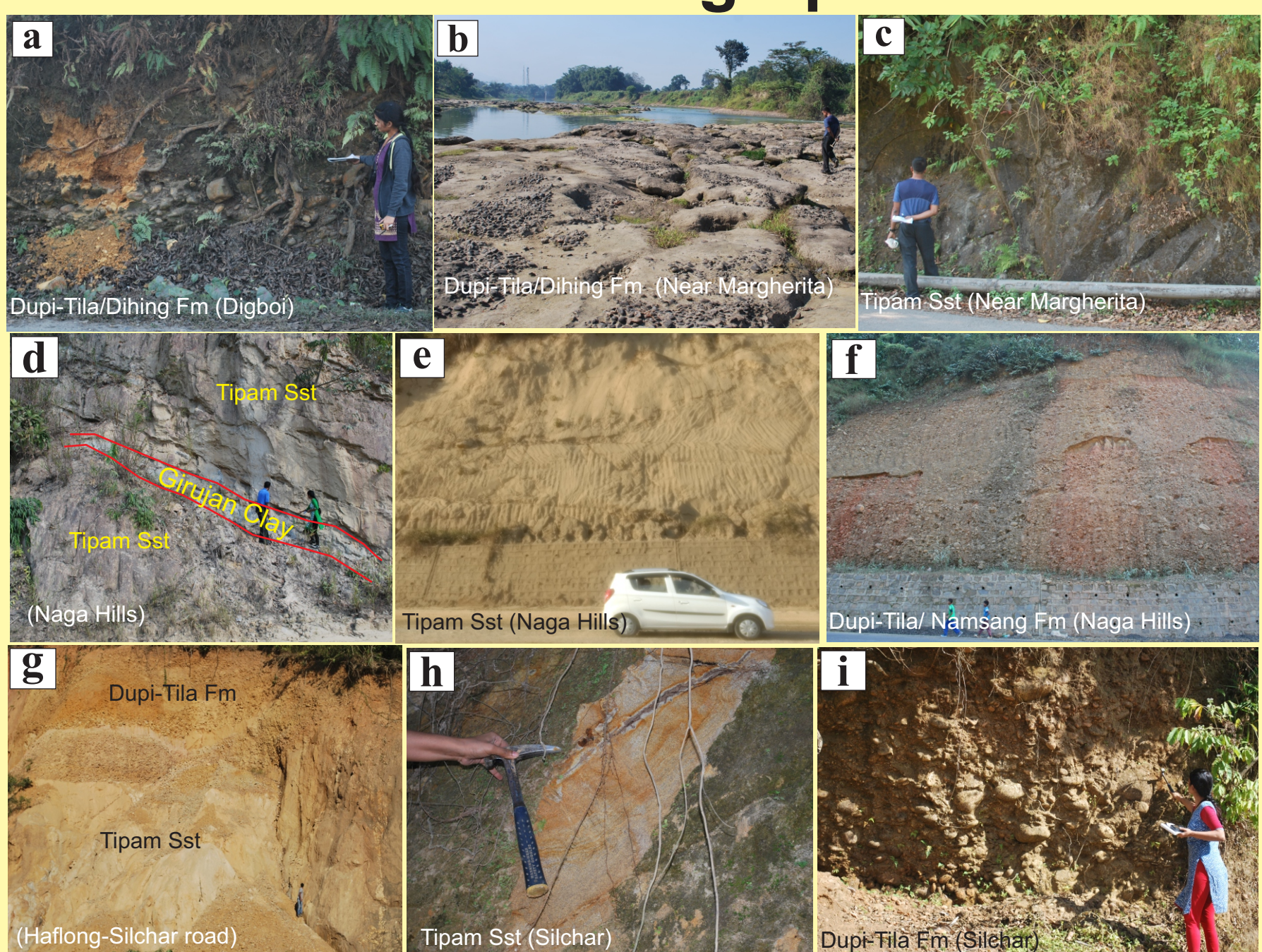
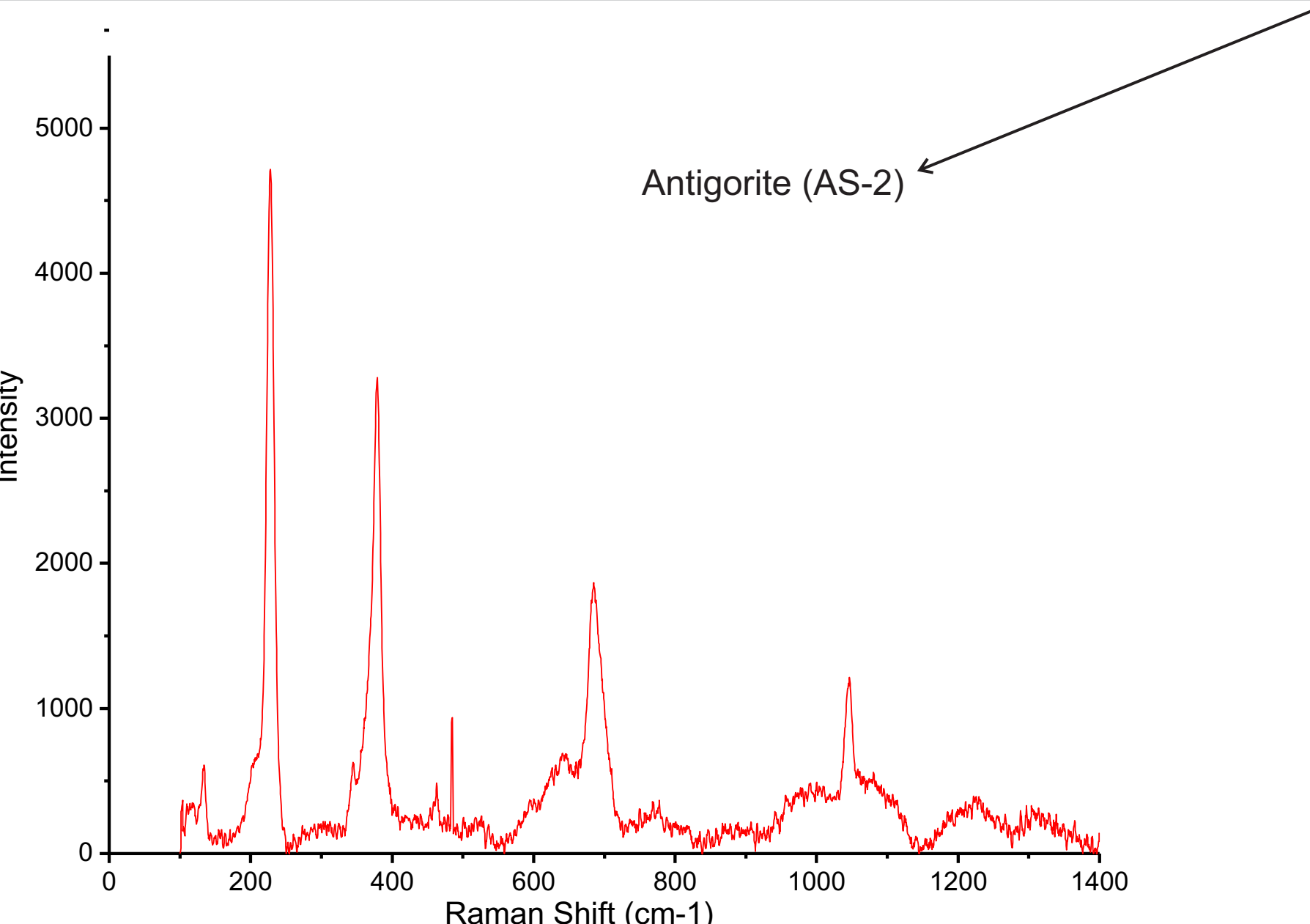


Fig.2 Outcrop photos showing Tipam sandstone (Upper Miocene-Pliocene unit) and the overlying younger Dupi-Tila/Namsang/Dihing (Upper Pliocene-Pleistocene units) fluvial successions of Assam-Arakan Basin.



Raman data confirms antigorite (a variety of serpentine mineral) and EPMA analysis of heavy minerals reveals presence of olivine (Mg-rich) mineral in AS-2.

Semi-quantitative analysis of heavies shows 31.7% olivine in the same unit. These observations indicate presence of serpentinite rock as a source in the provenance.

Detrital Zircon Geochronology

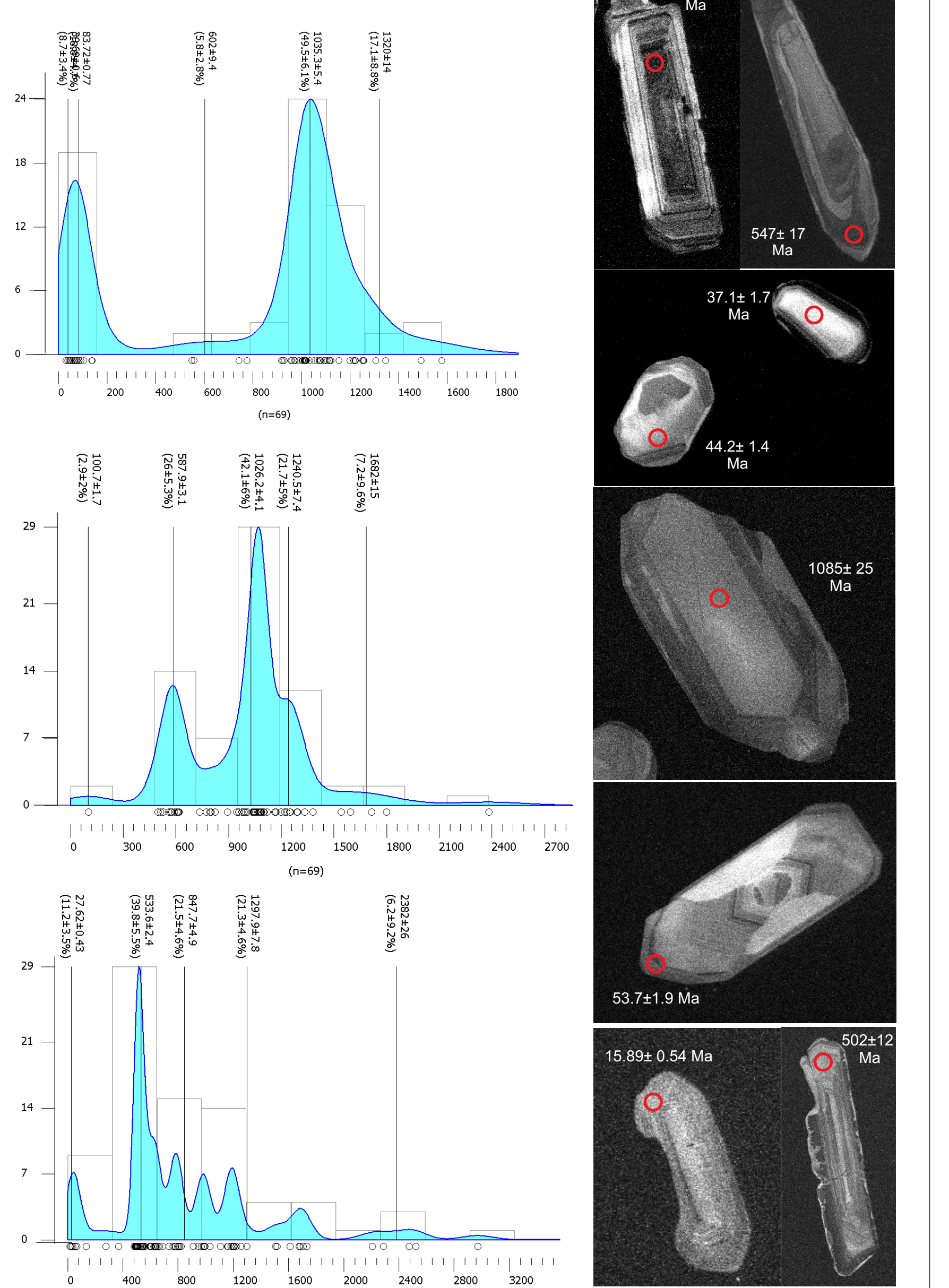


Fig.8 Kernel density plots of detrital zircon U-Pb ages from the analysed samples of Assam-Arakan Basin.

Methodology

- Petrographic observation
- Heavy Mineral study using semi-quantitative, XRD and EPMA analyses
- Detrital zircon U-Pb dating

Results

Petrography

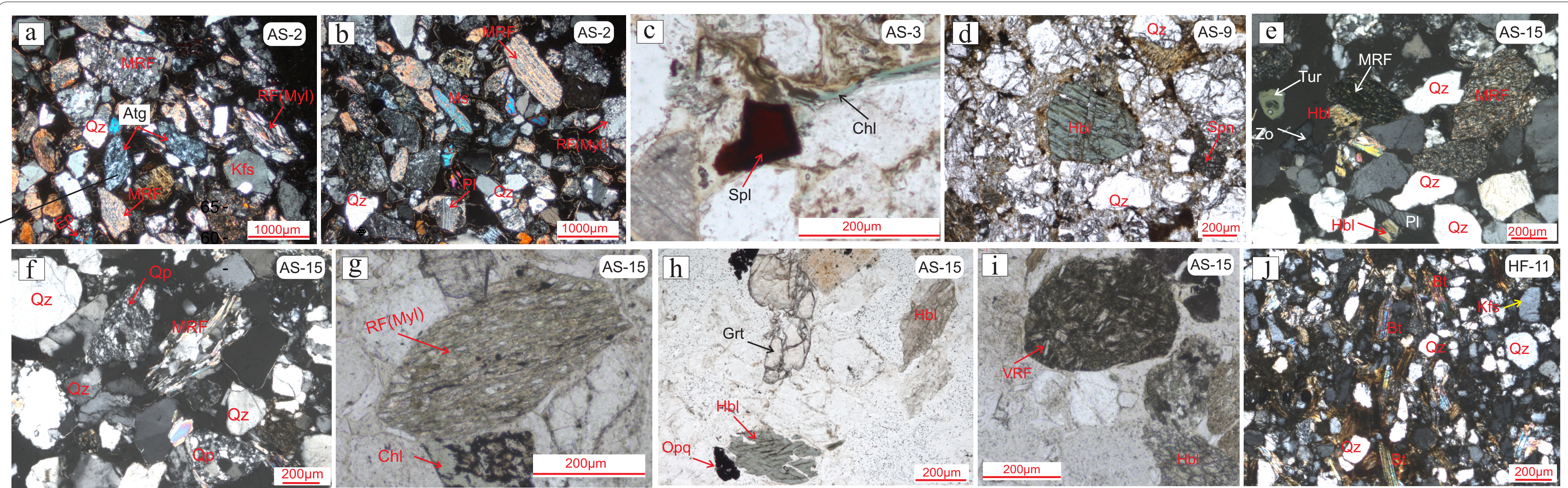


Fig.3 Petrographic study showing photomicrographs of different minerals and rock fragments observed from Neogene-Quaternary deposits of Assam-Arakan Basin. Qz- quartz, Kfs- K-feldspar, MRF- metamorphic rock fragment, Atg- antigorite, Ep- epidote, Myl- mylonite, Pl- plagioclase, Ms- muscovite, Spl- spinel, Chl- chlorite, Hbl- hornblende, Spn- sphene, Tur- tourmaline, Zo- zoisite, Qp- polycrystalline quartz, grt- garnet, opq- opaque, VRF- volcanic rock fragment, Bt- biotite.

Heavy Mineral Study

Table.1 Normalized percentage of heavy minerals in fluvial deposits of Assam-Arakan Basin.

| Minerals | Heavy mineral assemblages in the studied samples | | | | | | | | | | | | |
|--------------------|--|---------|------|-------|-------|-------|--------------------------------|------|------|---------|-------|-------|-------|
| | Tipam unit | | | | | | Dupi-Tila/Namsang/Dihing units | | | | | | |
| | AS-3 | AS-6(B) | AS-9 | AS-15 | AS-18 | HF-11 | AS-1 | AS-2 | AS-5 | AS-6(A) | AS-14 | AS-19 | HF-12 |
| Zircon | 5.0 | 3.6 | 3.9 | 2.1 | 1.6 | 9.9 | 7.0 | 1.5 | 11.4 | 31.0 | 31.7 | 6.4 | 7.7 |
| Tourmaline | 2.6 | 6.2 | 9.7 | 5.6 | 4.4 | 11.3 | 1.2 | 2.0 | 3.6 | 8.6 | 13.9 | 7.6 | 23.2 |
| Rutile | 1.6 | 5.8 | 0.9 | 0.7 | 2.5 | 3.7 | 3.3 | 7.0 | 5.4 | 18.1 | 18.4 | 7.0 | 12.0 |
| Garnet | 9.4 | 1.9 | 5.6 | 32.0 | 5.0 | 2.2 | 1.6 | 4.9 | 4.2 | 0.9 | 0.0 | 0.6 | 0.0 |
| Epidote Group | 33.9 | 21.6 | 16.4 | 3.5 | 16.9 | 23.2 | 29.6 | 9.0 | 7.2 | 11.2 | 0.6 | 22.3 | 9.4 |
| Sphene | 12.3 | 10.1 | 7.2 | 3.5 | 7.2 | 5.7 | 3.7 | 4.7 | 5.4 | 5.6 | 6.6 | 3.2 | 9.4 |
| Pyroxene | 3.9 | 9.1 | 9.9 | 5.9 | 9.4 | 9.9 | 10.3 | 16.6 | 1.2 | 3.0 | 3.9 | 3.2 | 3.0 |
| Amphibole | 0.0 | 7.9 | 24.2 | 29.6 | 20.3 | 12.1 | 1.6 | 2.0 | 0.0 | 0.9 | 0.0 | 0.6 | 5.2 |
| Aluminosilicates | 5.7 | 21.3 | 11.6 | 9.4 | 17.4 | 8.4 | 7.8 | 8.7 | 6.0 | 4.7 | 3.6 | 5.7 | 5.2 |
| Staurolite | 0.0 | 2.4 | 0.7 | 3.2 | 2.8 | 0.7 | 0.8 | 0.3 | 0.0 | 1.3 | 0.0 | 0.0 | 0.0 |
| Nioba | 2.3 | 3.4 | 2.2 | 0.2 | 1.9 | 2.7 | 23.0 | 1.5 | 6.6 | 6.9 | 15.4 | 34.4 | 13.7 |
| Chlorite | 3.9 | 1.0 | 0.9 | 0.9 | 0.0 | 6.4 | 2.1 | 0.3 | 25.7 | 0.0 | 0.0 | 0.0 | 3.4 |
| Chloritoid | 7.0 | 1.7 | 3.9 | 3.3 | 6.6 | 0.7 | 2.9 | 1.7 | 14.4 | 1.7 | 3.3 | 3.2 | 3.4 |
| Apatite | 4.7 | 1.2 | 1.2 | 1.6 | 2.5 | 0.2 | 0.0 | 0.9 | 0.0 | 0.0 | 0.0 | 0.0 | 0.0 |
| Carbonate(Cal+Dol) | 4.4 | 1.2 | 1.0 | 0.0 | 0.0 | 0.7 | 0.0 | 0.0 | 0.0 | 0.0 | 0.0 | 0.6 | 0.0 |
| Spinel | 1.8 | 0.5 | 0.2 | 0.2 | 0.3 | 0.5 | 2.5 | 1.5 | 6.6 | 4.3 | 0.0 | 0.6 | 0.9 |
| Olivine | 0.0 | 0.0 | 0.0 | 0.0 | 0.0 | 0.0 | 0.0 | 31.7 | 0.0 | 0.0 | 0.0 | 0.0 | 0.0 |
| Monazite | 0.0 | 0.0 | 0.0 | 0.0 | 0.0 | 0.2 | 0.0 | 0.0 | 0.0 | 0.0 | 0.0 | 0.0 | 0.0 |
| ZTR Index | 9.8 | 16.3 | 15.0 | 8.5 | 10.1 | 25.8 | 15.0 | 10.6 | 21.8 | 62.0 | 76.3 | 32.0 | 49.8 |
| Opaque mineral | 9.9 | 13.1 | 4.7 | 6.4 | 5.9 | 19.9 | 34.0 | 28.6 | 63.3 | 41.0 | 43.3 | 43.7 | 59.4 |
| Unknown | 0.5 | 1.2 | 0.5 | 0.0 | 1.3 | 1.5 | 2.5 | 5.8 | 2.4 | 1.7 | 1.8 | 5.1 | 3.4 |

Tourmaline Binary Plot

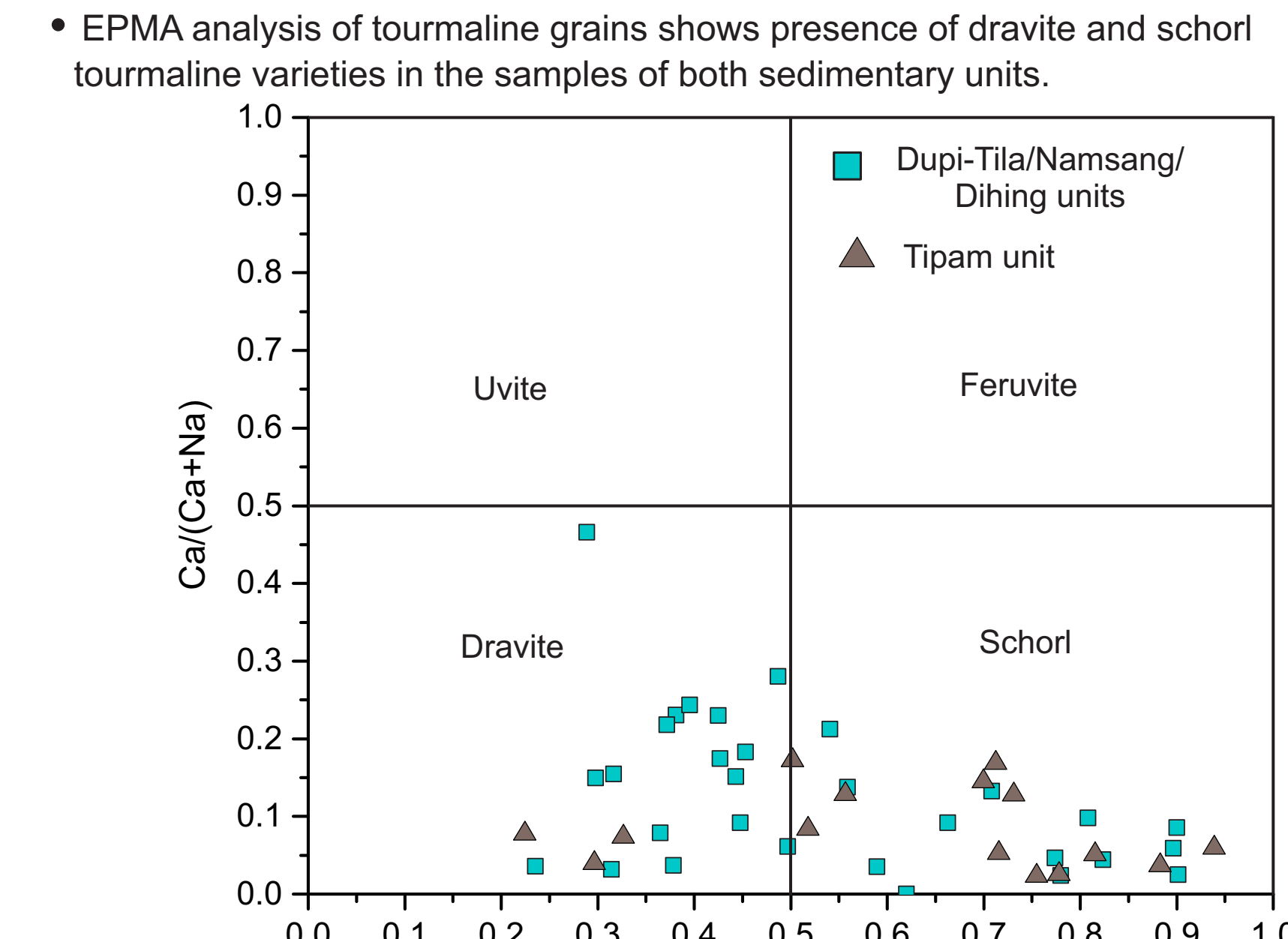


Fig.6 Fe/(Fe+Mg) vs Ca/(Ca+Na) binary plot represent tourmaline composition diagram (modified after Selway et al., 1998,2000; Kettanah et al., 2015).

Conclusions

- Petrography shows presence of many lithic fragments along with various heavy minerals such as epidote group mineral, tourmaline, spinel, garnet, chlorite, staurolite, hornblende in Tipam units. The observed mylonitic rock fragments, spinel, many epidote grains and antigorite mineral grains in younger units indicate its derivation from the lithologies exposed in Lohit-Dibang valley.
- Heavy mineral suits (Table-1) of both the units are almost similar with slight variation in the abundance of few minerals. Mineral such as garnet, amphibole, aluminosilicate, apatite are more in Tipam unit than its overlying younger unit, however, spinel and opaque minerals have high percentage in younger unit than Tipam unit.
- Mineral chemistry of heavies such as garnet, tourmaline and spinel indicates almost same mineral composition and hence the similar provenance history.
- Spinel geochemistry indicates the peridotitic and volcanic rocks as the source for detrital spinel in fluvial deposits of Assam Arakan Basin. Tidding suture zone of eastern Himalaya drained by the Dibang and Lohit drainages are proposed as the source for providing chrome spinel in both fluvial deposits of basin as suture zone rocks are the host for spinel minerals.

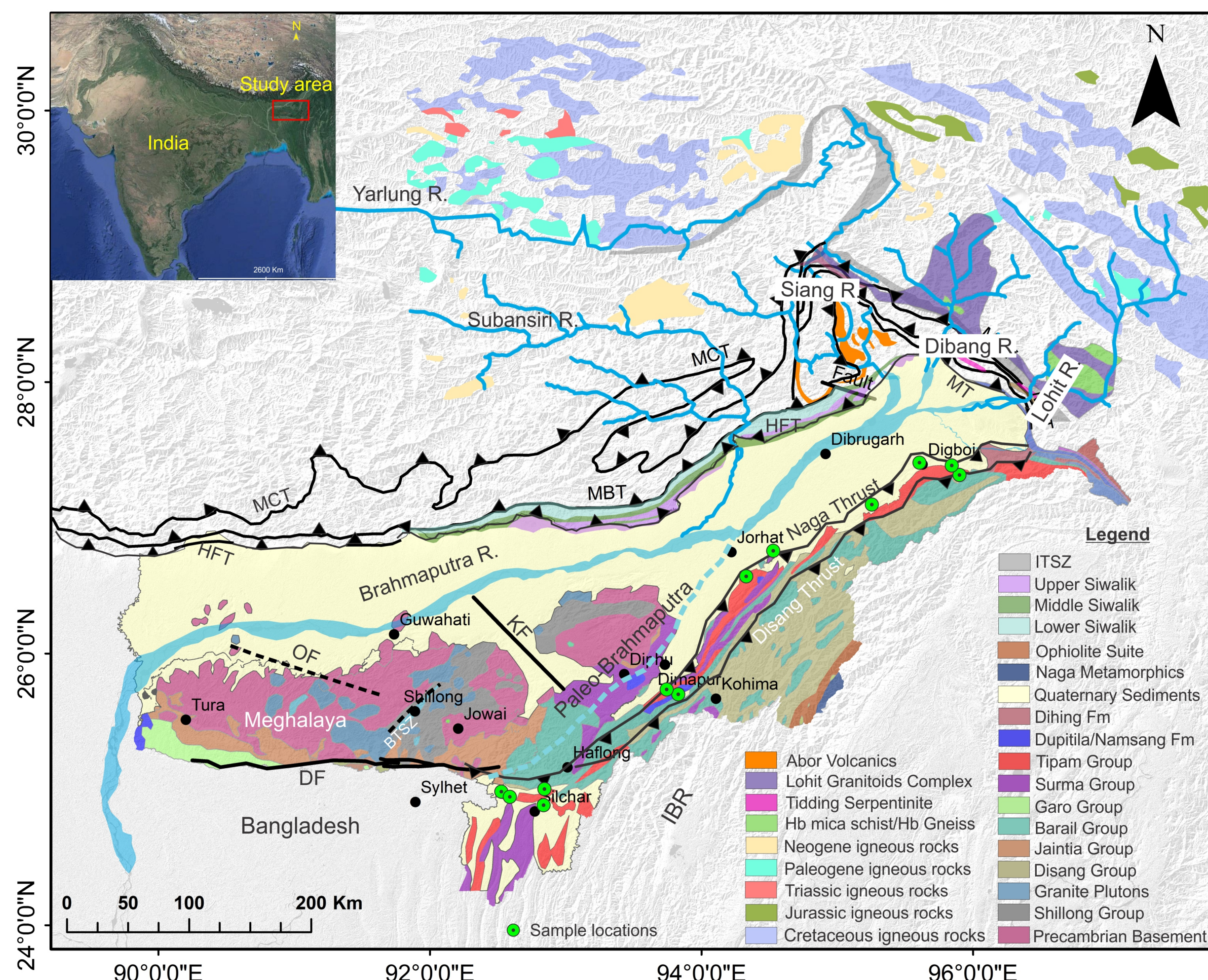


Fig.1 Geological map of the study area and adjoining regions (modified after GSI (1998; 2010); Biswas et al., 2007; Lang and Huntington, 2014). Red box in google earth image of India shows the location of study area. Sample locations are indicated by green circles. OF- Oldham fault, DF- Dauki fault, KF- Kopalai fault, BTSZ- Badapani-Tyrsad shear zone, ITSZ- Indus-Tsangpo suture zone, MT- Mishmi thrust, R- Rivers.

EPMA Analysis

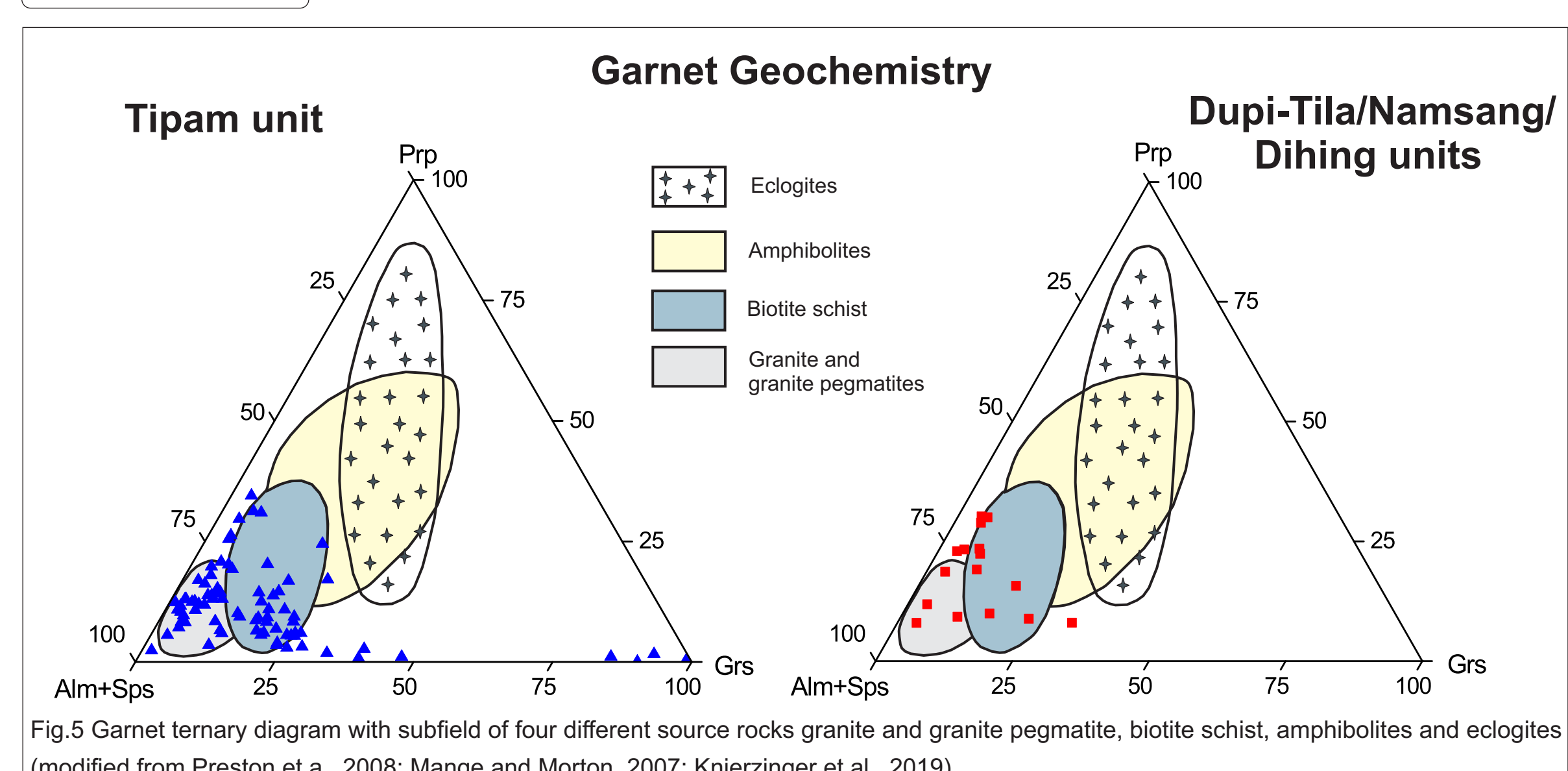


Fig.5 Garnet ternary diagram with subfield of four different source rocks granite and granite pegmatite, biotite schist, amphibolites and eclogites (modified from Preston et al., 2008; Munge and Morton, 2007; Kniezinger et al., 2019).

Spinel Geochemical Plot

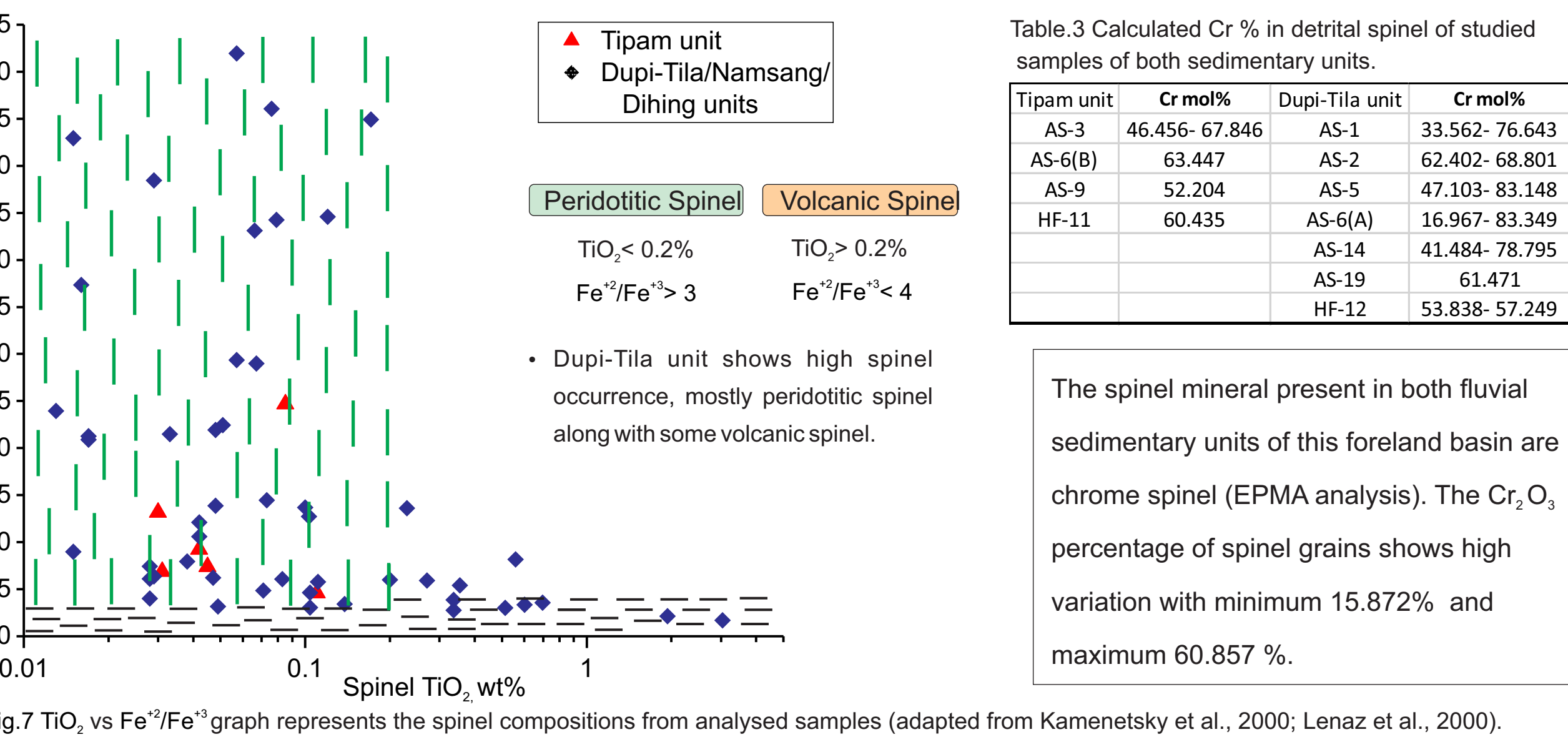


Fig.7 TiO₂ vs Fe²⁺/Fe³⁺ graph represents the spinel compositions from analysed samples (adapted from Kamenetsky et al., 2000; Lenaz et al., 2000).

XRD analysis performed to detect mineral phases in the samples shows the presence of most of the minerals identified by counting data and EPMA analysis. For example the presence of olivine in AS-2 sample and spinel records mainly in younger units support our observations.

- Results from petrography and heavy mineral study indicate Lohit- Dibang valley rock types as the probable source terrain.
- Initial analysis of detrital zircon U-Pb ages from studied samples reveals major age peaks at around 500 Ma and 1025 Ma with young ages between 16 Ma and ~140 Ma. These samples do not provide ages < 10 Ma, signifying the sediments not derived from Namche Barwa massif, eroded by the Tsangpo-Siang- Brahmaputra river system.
- It indicates that paleo-Brahmaputra seems not the cause for Assam-Arakan Basin deposits at least during the Pleistocene. Therefore, we tentatively propose that the Tipam and the younger Dupi-Tila/Namsang/Dihing units in the Assam-Arakan Basin were probably deposited by drainage flowing from Lohit- Dibang valley.

Acknowledgement- Authors are thankful to Department of Earth Sciences and IIT Bombay for their support. We also thank IUAC, Delhi for providing LA-ICP-MS facility to perform the detrital zircon U-Pb dating of the samples.